ResearchGate

See discussions, stats, and author profiles for this publication at: https://www.researchgate.net/publication/260251244

Simulations of Light Absorption of Carbon Particles in Nanoaerosol Clusters

ARTICLE *in* THE JOURNAL OF PHYSICAL CHEMISTRY A · FEBRUARY 2014

Impact Factor: 2.69 · DOI: 10.1021/jp412384j · Source: PubMed

CITATION
1

READS
52

5 AUTHORS, INCLUDING:

Thomas Hede
Stockholm University
14 PUBLICATIONS **80** CITATIONS
SEE PROFILE

Natarajan Arul Murugan
KTH Royal Institute of Technology
72 PUBLICATIONS **574** CITATIONS
SEE PROFILE

C. Leck
Stockholm University
148 PUBLICATIONS **3,771** CITATIONS
SEE PROFILE

Hans Agren
KTH Royal Institute of Technology
867 PUBLICATIONS **18,572** CITATIONS
SEE PROFILE

Available from: Hans Agren
Retrieved on: 26 January 2016

THE JOURNAL OF PHYSICAL CHEMISTRY A

Article

pubs.acs.org/JPCA

Simulations of Light Absorption of Carbon Particles in Nanoaerosol Clusters

Thomas Hede,[†] N. Arul Murugan,[‡] Jacob Kongsted,[§] Caroline Leck,[†] and Hans Ågren*[,‡]

[†]Department of Meteorology, Stockholm University, S-106 91 Stockholm, Sweden

[‡]Division of Theoretical Chemistry and Biology, School of Biotechnology, KTH Royal Institute of Technology, SE-10691 Stockholm, Sweden

[§]Department of Physics, Chemistry and Pharmacy, University of Southern Denmark, Campusvej 55, DK-5230 Odense M, Denmark

ABSTRACT: Black carbon soot (BS) is considered to be the second most contributing organic matter next to carbon dioxide for the global warming effect. There is, however, so far no consensus on the quantitative warming effect due to the increased distribution of black carbon in the atmosphere. A recent report (*Science* **2012**, *337*, 1078) suggests that due to BS there is only a few percentage enhancement in absorption of BS-immersed aerosols. To get proper interpretation of the available experimental data, it becomes essential to obtain details of the microscopic origin of the absorption and scattering processes of the aerosol clusters due to the presence of soot. However, so far, due to the large spatial scale and the need for a quantum mechanical description of the particles involved in the absorption and scattering, this quest has posed an insurmountable challenge. In the present work we propose the use of a multiscale integrated approach based on molecular dynamics and a quantum mechanical−molecular mechanical method to model the optical property of molecules immersed in nanosized aerosol particles. We choose fluoranthene (FA) with varying *cis*-pinonic acid (CPA) impurity concentration as an illustrative example of application. We observe that normally FA tends to be on the surface of the nanoaerosols but in the presence of CPA impurities its spatial location changes to a core aggregate to some extent. We find that the absorption maximum is only slightly red-shifted in the presence of increased CPA concentrations and that the oscillator strengths are not altered significantly. The comparable values for the oscillator strengths of all the low energy excitations suggest that the absorption enhancement of the aerosol due to BS will not be substantial, which is in line with the recent experimental report in *Science*.

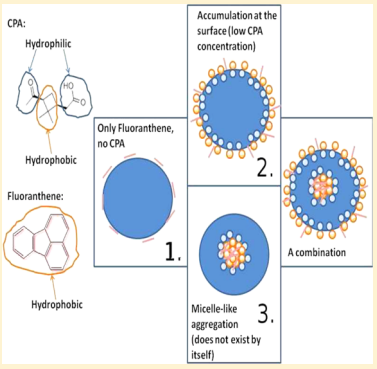

1. INTRODUCTION

Soot, referred to as light absorbing carbon particles, is considered as a key factor in the global energy balance as it can absorb incoming solar radiation and thereby warm the troposphere. Soot is even considered to be equally important as a warming factor as carbon dioxide.[1−4] In this study we investigate the chemical compound fluoranthene (FA) as a model for soot. FA absorbs in the UV-spectral region[5] and is a simple polycyclic aromatic hydrocarbon (PAH) consisting of three benzene rings merged together with a five-carbon ring yielding a planar structure. PAHs are known to form as an incomplete combustion product in diesel engines and other similar combustion processes.[6−8] PAHs are part of soot particles emitted from biomass burning, motor traffic, and many industrial processes.[9] To understand the impact on the radiation absorbance, it is vital to study the process of aging of the carbon particles. Aging means that the soot changes surface character from hydrophobic to more hydrophilic through mixing and chemical reactions during transport with winds in the troposphere. Freshly emitted soot has an open and branched, fractal-like structure[10] and is about 20−60 nm in diameter.[11] During the aging, the soot combines with other types of compounds and forms a more spherical form. Examples of such compounds are secondary organic aerosol (SOA) particles. SOA particles can form through oxidation of α-pinene emitted from vegetation[12] and even from the oceans.[13,14] It has been shown that carbon particles made from fluoranthene can be solubilized into aggregates of SOA in nanosized water droplets.[15,16] This implies that hydrophobic carbon particles and soot-like substances more easily can be taken up into aerosol and cloud droplets. Without the presence of a core, a cloud condensation nucleus (CCN), the critical supersaturation needed for droplet growth is much more than 100% relative humidity, but if there is some material, inorganic or organic, the critical supersaturation can be much lower, according to Köhler theory.[17] *cis*-Pinonic acid (CPA), a SOA, can act as CCN. CPA is also a strong natural surfactant, as it has amphiphilic properties; CPA therefore is surface-active and can decrease the surface tension[16,18−20] of aerosol particles and cloud droplets. The surface tension is affected and most probably enhanced by the uptake of carbon particles.[15] Moreover, the orientation of the FA molecules on the surface is affected by the presence of CPA.[15] The spatial location (i.e., whether it is on surface or in the core) and orientation may be

Received: December 18, 2013
Revised: February 18, 2014
Published: February 18, 2014

ACS Publications © 2014 American Chemical Society

dx.doi.org/10.1021/jp412384j | *J. Phys. Chem. A* 2014, 118, 1879−1886

of importance for the absorption properties and computation of this is the subject of the present study.

Even though FA is considered to be potentially carcinogenic, its derivative compounds have a number of useful electronic properties suitable for many applications related to energy and technology. For example, it is often used as a spacer molecule in dye sensitized solar cells.[21] In addition, quenching in the substituted FAs due to molecules such as dioxygen, sulfur dioxide, and nitro compounds has been utilized in sensing application of explosives and other chemicals.[22−24] The optical properties of FA and other polycyclic aromatic hydrocarbons, in particular the solvent induced shifts in absorption and emission,[5,25] have been studied in some detail experimentally and theoretically.[26] The first absorption spectra for FA, reported by Edgar Heilbronner as early as 1966,[5] identifies four major bands appearing at 359, 324, 286, and 262 nm in ethanol solvent. A small red shift is reported in the case of benzene solvent, which has been attributed to the formation of a weak intermolecular complex between benzene and FA.[25] As far as the emission spectra are concerned, the fluorescence intensity is affected by a number of compounds. For example, compounds such as sulfur dioxide quench the fluorescence intensity of the emission band appearing at 462 nm.[24] The optical properties were also explored using semiempirical and ab initio computational approaches. In particular, time-dependent density functional theory and real-time-dependent density functional theory were recently used to characterize different bands observed in the absorption spectra of FA[26] but these studies were limited to a single molecule without accounting for the environmental effect. In this article, we study optical properties of FA[26] embedded in a nanosized water droplets using recent multiscale computational techniques. First, we model the finite temperature structure of an organic mixture of FA and CPA dissolved in a water droplet using molecular dynamics (MD). We use various configurations selected from the MD trajectory for computing the optical properties of FA using the so-called integrated approach where the structure and properties are modeled using different computational methods. Below we discuss the structure and optical properties of FA and draw some conclusions and ramifications from the results.

2. COMPUTATIONAL DETAILS

MD simulations are used to simulate the structure, dynamics, and interacting forces of our model systems. The intermolecular forces are described by a force field as detailed below. The initial setups of systems were generated by the Groenigen Machine for Computer Simulations (GROMACS) utility genbox.[27,28] The FA molecules were randomly inserted in a box of length 7.3 nm. CPA model molecules were further inserted in this box, along with 10 000 water molecules. We used the common extended simple point charge (SPC/E) model for water solvent.[29] Each side of the simulation box was enlarged by 6 nm. This is done to avoid the interaction between the central simulation box and its images to create a vacuum-like environment. The usually employed periodic boundary condition (PBC) generates an imaginary infinite box size by repeating the box side by side in all directions, so that if a molecule exits the box at one side, an equivalent molecule enters the box from the opposite side. This is a useful condition when bulk solutions and periodic systems like molecular crystals and membranes are simulated, but for our spherical cluster simulations, the PBC is not suitable and the interaction of molecules in the central simulation box with its images in other boxes has to be removed. Even though it is possible to remove PBC in GROMACS, we have adopted a different approach. In the present case, such interaction between the molecules in the original simulation box and those in periodic images is removed by enlarging the simulation box. The system was energy minimized by the steepest descent and conjugate gradient methods implemented in GROMACS. After the minimization, the systems were simulated for 1 ns during which spherical cluster is formed spontaneously due to the minimized surface energy of a sphere. A canonical (*NVT*) ensemble was used with the temperature maintained at 286 K by the Nosé−Hoover thermostat[30] to best mimic atmospheric conditions. Bonds to hydrogen atoms were kept rigid by the Linear Constraint Solver, LINCS[27,31] algorithm. The optimized potentials for liquid simulations (OPLS) force field[32] has been used to describe the intermolecular interactions of the FA and CPA molecules. This force field is widely used for small molecules and the justification for using this for FA and CPA is discussed in our previous studies.[15,16,18] The time step for the integration of equation of motion was set to 2 fs. Many combinations of FA in CPA were studied using MD. Each system was hereafter simulated for 5 ns. On the basis of our earlier studies[16] we suggest that the total time scale employed is more than enough for equilibration and the formation of aggregates in the core. During the simulations, the trajectories were stored every 1 ps (500 steps) for further analysis. From the trajectory files, snapshots of the systems for a given time step were extracted and used for absorption calculations. As we will describe later, for some cases of FA nanoaerosol clusters, we used 80 configurations for averaging the absorption spectra whereas for the remaining systems, we used the last configuration of the trajectory.

The absorption spectral calculations are usually limited to systems of small size because a quantum mechanical treatment of the system is needed. However, in many of the solute−solvent systems[33−37] and chromophore−protein systems[38−41] the whole light absorption process is limited to a small fragment of the entire system and it is therefore sufficient to treat this part of the system quantum mechanically (which will be referred as the QM subsystem) and interactions between the two subsystems can be accounted for by including an interaction potential in the effective Hamiltonian of the QM subsystem. Such an approximation is implemented and used in many available hybrid quantum mechanics/molecular mechanics (QM/MM) methodologies, and in each of these approaches the interactions between the two subsystems are modeled differently. The one implemented in the recent version of Dalton is the most sophisticated one and accounts for electrostatic and polarization interaction between the two subsystems in the response (absorption) calculation.[42−44] In particular, we have used time-dependent density functional theory/molecular mechanics (TD-DFT/MM) calculations. For this purpose, we need to have the polarizable force field including charges and polarizabilities for all the molecules in the MM subsystem. The QM description has been used for FA whereas the MM subsystem can have three different types of molecules, namely, CPA, FA, and water. For CPA and FA, the charges were derived using the restrained electrostatic potential fit.[45] The electrostatic potential (ESP) used in the fitting was calculated at the B3LYP/aug-cc-pVTZ[46] level of theory using the Gaussian09[47] with tight SCF convergence criteria. The ESP grid consisted of ten concentric layers of points and about 2500

points per atom. The fitting was performed using the antechamber program from the AmberTools suite.[48] The isotropic polarizabilities were derived from anisotropic polarizabilities calculated at the B3LYP/aug-cc-pVTZ[46] level of theory using the local property (LoProp) procedure.[49] This basis set was recontracted to atomic natural orbital form as required by the LoProp approach. To maintain a comparable level of description for all the molecules in MM region, we have adopted the Ahlström force field[50] for water solvents which places charges on oxygen and hydrogen atoms and in addition an isotropic polarizability at the oxygen center. Overall, the absorption spectra calculations were carried out for the FA molecule using hybrid QM/MM response approach where the effective Hamiltonian accounts for its interaction with water, CPA, and FA molecules. The effect of media/environment decreases with increasing distance from the QM subsystem and so we have used a cutoff 15 Å to choose the solvent molecules to be included in the MM region of subsystem. Due to this reason, it is evident that the number of solvent molecules in the MM region varies quite significantly depending upon the position of FA (i.e., whether it is on the surface of the droplet or core). The changes in the environment topology usually have influence on the absorption property of solute molecule. The excitation energy calculations were carried out using density functional level of theory with the CAM-B3LYP functional[51,52] and the Turbomole-TZVP basis set.[53] However, coupled cluster (CC) and coupled-cluster/molecular mechanics (CC/MM) calculations have been performed at the level of CC2[54] using the aug-cc-pVDZ basis set.[46]

In addition to the aforementioned calculations carried out for the extended system that include FA, CPA, and solvent molecules, we have also carried out calculations for the single FA molecule where the solvent effect is accounted through polarizable continuum model.[55] The purpose of this set of calculations is to see the relative performance of the explicit solvent model when compared to the implicit solvent model. Moreover, this set of calculations correspond to zero temperature and so comparison also accounts for the contributions due to finite temperature effect.

3. RESULTS AND DISCUSSIONS

The main objective of this study is to investigate the absorbance by FA in nanosized water droplets with and without the presence of the organic natural surfactant CPA. We aim to determine the difference in absorption in the presence of CPA and to investigate the absorption dependency on concentration of FA in the clusters as well as the dependence on the molecular orientation and spatial location. The three different possibilities are (i) FA on the surface in a flat configuration (flat means a general perpendicular orientation toward the cluster center), (ii) FA on the surface solubilized by CPA in an up-ended configuration (up-ended means a general orientation in line with the cluster diameter), and (iii) FA in the core of the aggregate formed by CPA molecules. They are more or less randomly mixed and orientated. For the three different orientations, see Figure 1.

The starting point for calculations of absorption are cluster configurations from the MD trajectory containing water, FA, and CPA molecules. As we mentioned above, in some cases, 80 configurations from the trajectory were used whereas for other cases only the last snapshot of the MD has been used. Listed below are the different clusters (Table 1). The number of water molecules in all systems of Table 1 is 10 000.

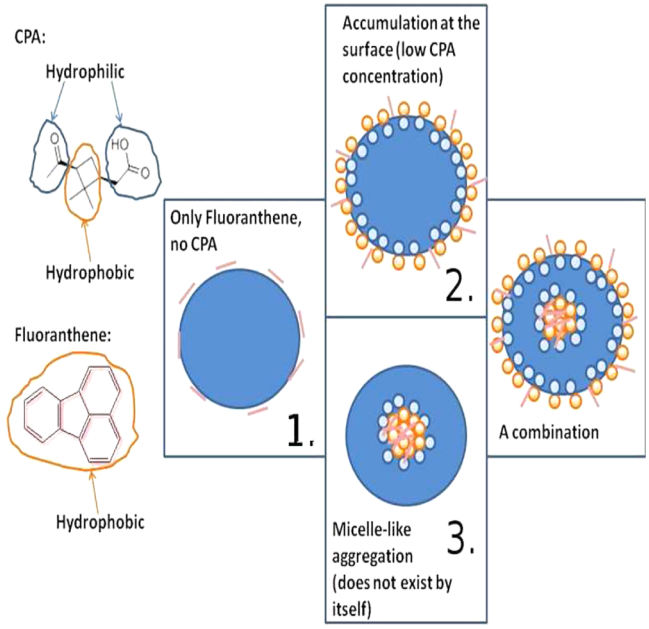

Figure 1. Molecular distribution in nanoaerosol clusters. An FA molecule is represented by a lilac stripe, and a CPA molecule is represented by an orange sphere and a blue sphere connected.

Table 1. The Various Systems Studied and the Distribution of FA Molecules between the Surface and Core Sites of a Nanoaerosol

system	CPA	FA	surface FA	core FA
1fa0cpa	0	1	1	0
13fa0cpa	0	13	11	2
7fa81cpa	81	7	6	1
13fa81cpa	81	13	10	3
27fa81cpa	81	27	16	11
1fa100cpa	100	1	1	0
10fa100cpa	100	10	7	3
20fa100cpa	100	20	19	1
30fa100cpa	100	30	21	9

The cluster systems listed in Table 1 were generated using MD simulations as detailed in the previous section. These simulations are of the same type as conducted in a previous study.[15] In Figure 2, we show a graphical representation of the configuration produced by the MD simulations of the system consisting of 20 FA molecules, 100 CPA molecules, and 10 000 water molecules. In Figure 2, water molecules are omitted to reveal the distribution of the FA and CPA molecules accumulated at the surface and in one aggregate.

As can be seen from Figure 2, the CPA molecules assemble on the surface and in one micelle-like aggregate in the center of the cluster. The orientations of FA molecules were determined by visual inspection of the trajectories. FA molecules that reside on the surface were never found to later migrate to the core and vice versa. The FA molecules are solubilized at the surface in an up-ended configuration as well as one FA molecule, in this particular case, solubilized in the micelle-like aggregate as a core. These findings were previously reported.[15] In the study by Hede et al., values for the surface tensions of some systems were reported. In this study we will not focus on this particular property (surface tension), even though it is of great importance for the condensational growth rate of nucleating

dx.doi.org/10.1021/jp412384j | J. Phys. Chem. A 2014, 118, 1879−1886

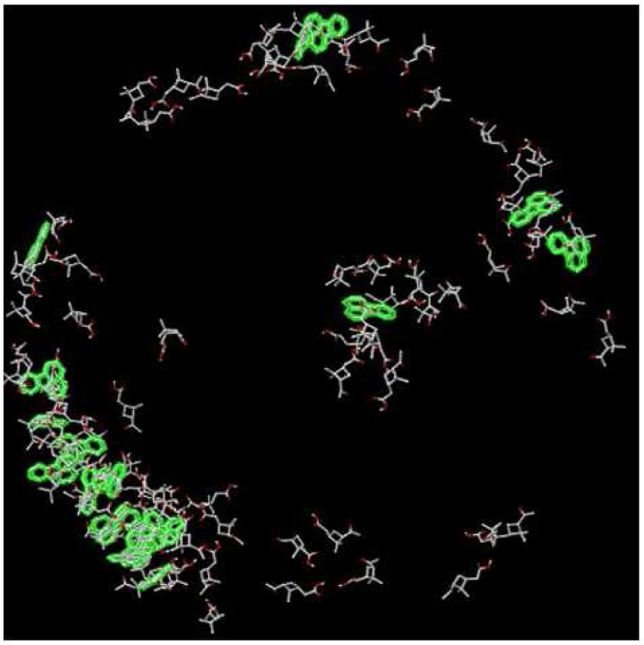

Figure 2. Cluster system 20fa100cpa. The figure is shown in a cross-sectional view, and the water molecules are removed for clarity. CPA molecules are gray and FA molecules are green.

water droplets, according to Köhler theory.[17] Moreover, surface tension has no impact on the light absorbing properties of either the CPA or FA, because it is associated with the orientation of the water molecules at the surface and the water molecules do not contribute essentially to the light absorption. We have computed the absorption spectra for FA in the clusters listed in Table 1 using the TD-DFT/MM response approach.[43,44] In all cases the FA molecule is treated at the density functional theory with CAM-B3LYP, a Coulomb attenuated exchange−correlation functional, whereas the remaining solvent (water, CPA, and in some cases FA) molecules are described using a polarizable molecular mechanics force field. When more than one FA is present in the cluster, the light absorbing property has been averaged over all such molecules; these results will be discussed in the latter section of the article.

Before discussing the absorption results based on the clusters, we consider here first the absorption results based on a more simple description of the system, i.e., a geometry optimized fluoranthene molecule embedded in a dielectric continuum mimicking the effect of the water solvent. We refer to these calculations as static because no dynamical effects are included in these dielectric continuum calculations. The dielectric continuum model chosen for these calculations is the PCM model.[55] It will be relevant to compare the results from this implicit solvent model with the results obtained from the explicit solvent model. In the former one (implicit) the solvent is described as a polarizable continuum; i.e., only the averaged effect of the solvent is considered, and this in turn is described by a polarizable medium characterized by a dielectric constant. In the latter case, as the name implies, the solvent molecules are treated explicitly and directional intermolecular hydrogen bonding between the solute−solvent system is thus included.

The results from the static calculations are presented in Table 2. In addition to the PCM based results we have also included results based on a geometry optimized FA molecule in isolation (vacuum). As can be seen, the oscillator strengths for excitations 2 and 4 are manifold larger than for the other two states. The absorption maximum computed for the gas phase and in water solvent differs by only 1−4 nm, i.e., a very small solvent effect. This small shift could be due to the incapability of the PCM model to account for the solvatochromic shift in fluoranthene. Another possibility is that fluoranthene does not exhibit any significant solvent-induced shift in its spectra. To verify this, we present below the results from TD-DFT and TD-DFT/MM calculations where the latter include the explicit solvent model. These calculations have been carried out for a single snapshot corresponding to the 1fa0cpa system, and the results are presented in Table 3.

Table 2. Lowest Four Excitation Energies (nm) and Corresponding Oscillator Strengths (in Parentheses) Calculated for an Optimized FA Geometry Optimized in Gas Phase and in Water Solvent[a]

excited state	in vacuum	in water solvent
1	371 (0.004)	369 (0.006)
2	348 (0.169)	352 (0.244)
3	300 (0.028)	301 (0.045)
4	271 (0.154)	272 (0.223)

[a]The PCM model is used for the solvent description. The results presented here are based on TD-DFT and TD-DFT/PCM approaches carried out at the B3LYP/TZVP level of theory.

Table 3. Absorption Maximum (nm) and Oscillator Strength (in Parentheses) for the 1fa0cpa System Computed from TD-DFT and TD-DFT/MM Methods and Compared to Results from CC and CC/MM Methods

method	state 1	state 2	state 3	state 4
TD-DFT	375 (0.01)	345 (0.2)	301 (0.04)	263 (0.2)
TD-DFT/MM	366 (0.04)	344 (0.2)	301 (0.05)	261 (0.2)
CC	372 (0.01)	352 (0.2)	319 (0.03)	276 (0.3)
CC/MM	364 (0.06)	351 (0.2)	318 (0.04)	274 (0.3)

The calculations for the large clusters will be based on TD-DFT due to the large number of systems studied, which prohibits the use of more accurate computational approaches such as CC. However, to check the reliability of the TD-DFT based results, we have carried out excitation energy calculations for the 1fa0cpa system using the CC and CC/MM approaches.[56] Note that the TD-DFT results in Tables 2 and 3 differ due to the use of a geometry optimized structure in Table 2 whereas in Table 3 we have used the structure for fluoranthene as extracted from the MD simulation. The CC based calculations in Table 3 are seen to display a similar trend as in the case of the TD-DFT based approach, thereby validating the latter approach. Comparing with the PCM based results in Table 2, we observe a much larger solvent effect on, e.g., excitation number 1. However, care should be taken in a direct comparison between the solvent effects predicted from the implicit and explicit solvent models because the latter only includes a single configuration and thus neglects averaging of several configurations. Still, the results in Table 3 indicate that account of specific solute−solvent interactions may be of significant importance. Having now discussed the reliability of our computational procedure, i.e., electronic structure method and solvent model, we present in Table 4 the excitation

Table 4. Absorption Maximum (nm) and Oscillator Strength (in Parentheses) for the Lowest Four Excitations of FA[a]

system	state 1	state 2	state 3	state 4
1fa0cpa	366 (0.039)	344 (0.233)	301 (0.045)	261 (0.182)
13fa0cpa	375 (0.082)	349 (0.201)	294 (0.045)	265 (0.218)
7fa81cpa	380 (0.019)	358 (0.271)	297 (0.039)	265 (0.216)
13fa81cpa	382 (0.053)	353 (0.224)	298 (0.046)	267 (0.229)
27fa81cpa	379 (0.058)	351 (0.236)	296 (0.057)	268 (0.253)
1fa100cpa	380 (0.034)	353 (0.241)	296 (0.048)	267 (0.241)
10fa100cpa	381 (0.043)	354 (0.231)	296(0.042)	267(0.024)
20fa100cpa	372 (0.059)	351 (0.233)	296 (0.051)	267 (0.240)
30fa100cpa	379 (0.030)	356 (0.264)	296 (0.051)	267 (0.233)

[a]The results are based on the TD-DFT/MM approach.

energies and the associated oscillator strengths computed for FA in the systems previously listed and based on the MD simulations.

These calculations aim at showing the concentration dependence of the absorption spectra and the absorption cross sections (related to oscillator strengths) of FA. As we have shown, when there are no CPA molecules in the water droplet, FA prefers to be on the surface. MD simulations performed by Hub, Caleman, and van der Spool have shown that hydrophobic compounds have a large surface preference.[57] This is also clearly seen from the results presented for various clusters as in Table 1, which shows that a large number of FA tends to remain on the surface of the cluster. However, FA molecules can be solubilized to some extent into the aggregate core when there are CPA molecules present.[15] In the present study we aim to understand whether there are any differences in the absorption properties of FA when it is in the aggregate core or on the surface. As can be seen in Figure 3a,b, the number of solvent molecules accessible to FA is largely diminished when it is on the surface and the solvation shell structure is altered to a large extent.

Probably, this difference should also affect the absorption spectra of FA, and to investigate this, we have calculated the four lowest energy excitations – the results are presented in Table 4. Interestingly, as it can be seen, the absorption maximum and absorption cross sections do not show any particular FA concentration dependence. A small red shift in the first excitation is seen when CPA molecules are included in the water droplet (see the case of 1fa0cpa and 1fa100cpa systems and 13fa0cpa and 13fa81cpa systems). However, as mentioned above, this transition is in fact the one that carries the smallest oscillator strength and is therefore in this respect the less interesting state. The results presented in Table 4 are from averaging over the total number of fluoranthene molecules in a given snapshot from the trajectory. It is also possible to compute the absorption property of an FA molecule as a time average. However, due to the computational cost involved, we have just computed the time evolution of absorption maximum for a single FA molecule in the 10fa100cpa system – the results are shown in Figure 4.

The instantaneous and N-point averages of the absorption maximum (corresponding to the first excitation) values are shown as a function of number of configurations. As it can be shown, at least averaging over 30–40 configurations is needed to get the convergence of the absorption maximum, and this is the case for a single fluoranthene molecule. The computed standard deviation in excitation energy is 0.18 eV, and the standard error associated with the first excitation energy is only 0.02 eV. However, there is a critical problem with the time

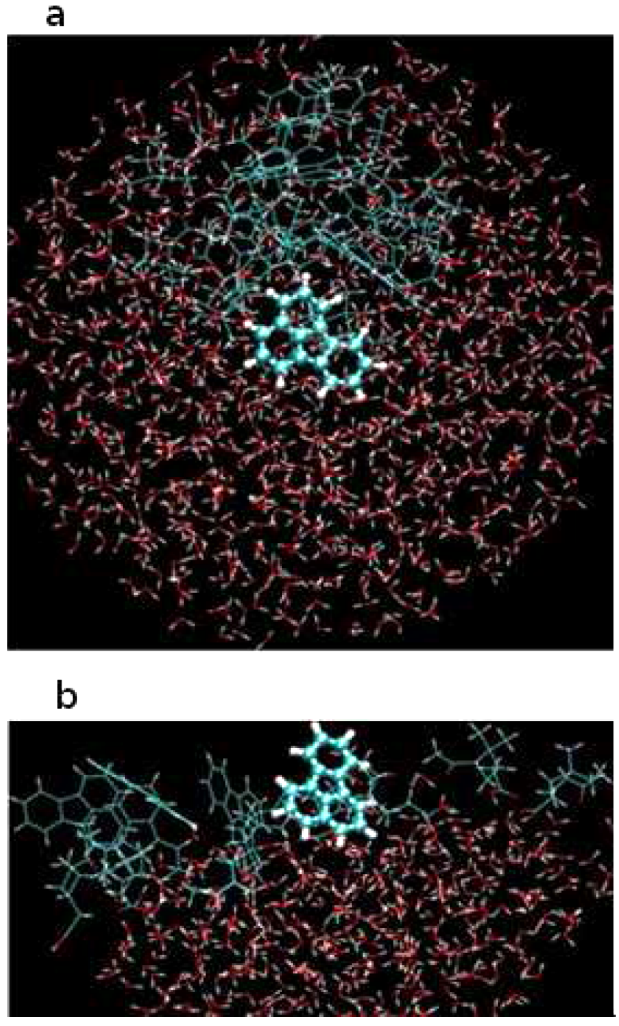

Figure 3. FA in the core (a) and surface of droplet (b) corresponding to the 27fa81cpa system. The molecules within 15 Å from the FA molecule are shown in this figure.

averaging. For example, if the selected FA remains just in the core or just on the surface, then the value computed does not represent the actual value of the ensemble of FA molecules. The computed time average of absorption maximum corresponding to the first excitation is 381 nm (the oscillator strength 0.043) which in fact differs with the ensemble average reported in Table 4. This we attribute to the possibility that the given FA can be on the surface or in the core and so the computed time average for these two cases may be slightly different. We have already shown that in the case of the

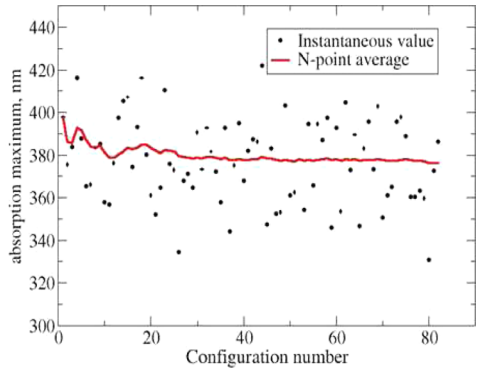

Figure 4. Instantaneous and N-point average of the absorption maximum.

10fa100cpa system, there are 7 FA molecules at the surface and 3 FA molecules in the core (refer to Table 1). So, the ultimate method for computing the light absorption property is to take the average from both time and ensemble averages, which will be computationally very demanding. Given the situation that the FA can be in the core or in the surface, it would be reasonable to rely on the ensemble average, which is computationally feasible and is advantageous for the cases where the FA molecules are spatially distributed between the core and surface sites of the aerosol cluster.

4. CONCLUSIONS

The present work is motivated by the important role that organic substances in water clusters, and in particular soot and soot-organic composites, play in the radiation balance of the atmosphere. It takes advantage of recent advances of multiscale modeling techniques (QM/MM) for modeling optical properties and spectra of molecular systems embedded in complex heterogeneous environments which now allows acquiring microscopic, even atomically resolved, prediction and understanding of such effects. As there is a lack of knowledge of more precise distribution of chemical content of the atmospheric particles, we are retained to work with model systems when the QM/MM method is applied. Here we chose to study fluoranthene and *cis*-pinonic acid as representatives for polycyclic hydrocarbons and organic coabsorbents, respectively. Our conclusion is 2-fold. The first part refers to the methodology itself: We have shown that the integrated molecular dynamics and hybrid QM/MM response approach can be used to model well the optical properties of polycyclic aromatic hydrocarbons or soot-organic particles embedded in the water droplet along with organic coabsorbents. By choosing a relatively small model molecule for the PAH, we have been able to very precisely validate the applied TD-DFT (vacuum) or TDDFT/MM (embedding) approach by the high level ab initio coupled cluster method (CC, respectively, CC/MM). As most future atmospheric applications of the present kind will refer to the TD-DFT/MM model, this validation is very encouraging. The second conclusion refers to the studied systems and their optical properties. We find that the PAH molecules tend to remain on the surface of the water droplets revealing their hydrophobic nature. However, CPA, having both a hydrophobic and a hydrophilic group, assists to some extent in the internalization (solubilization) of FA to the core aggregate of the water droplet. Although the spatial distribution of FA is significantly perturbed by the CPA concentration, the optical properties of the FA are not significantly altered either by the concentration or by the position in the cluster. Neither the static TD-DFT/PCM nor the dynamic TD-DFT/MM calculations suggest that there is any significant solvent effect on the excitation energies of FA. In regard to the CPA coadsorption, we also report rather insignificant change. We have also discussed the two different ensemble and time-average procedures for averaging. Given the situations that the FA can be just on the surface or in the core, the ensemble averaging might yield comparable results with the realistic system. The statistics indicate that the standard errors are within 0.02−0.04 eV for these two averaging procedures, the results have to be carefully analyzed if the environment-dependent shift in the OPA spectra and the absorption cross section is not very significant. The results indicate that neither the structural composition of the composites in the water clusters nor the coabsorption itself changes significantly the FA absorption properties in the atmosphere in terms of wavelength and oscillator strength. The current study supports the recent experimental study, which reports that the black carbon in the atmosphere does not contribute to the warming effect.[58]

5. OUTLOOK

The effect of aging of the carbonaceous aerosol particles are of importance as PAH molecules can be oxidized by ozone and hydroxyl radicals to form more soluble products. These oxidation products may in turn interact more strongly with the coabsorbent and the solvent. Here, a more detailed polarizable model would be able to show stronger absorption effects, which is a future objective. Another important property of atmospheric aerosol particles is the elastic light scattering, and here we intend to apply our multiscale modeling approach also to encompass that important effect concerning PAHs and other soot-like substances. We thereby hope to come closer to describing the direct effect of carbonaceous aerosol particles, which poses one of the largest uncertainties of the radiation balance of planet Earth.

■ AUTHOR INFORMATION

Corresponding Author

*H. Ågren: e-mail, agren@theochem.kth.se.

Notes

The authors declare no competing financial interest.

■ ACKNOWLEDGMENTS

This work was supported by a grant from the Swedish Infrastructure Committee (SNIC) for the project "Multiphysics Modeling of Molecular Materials", SNIC025/12-38. J.K. thanks the Danish Center for Scientific Computing (DCSC), The Danish Councils for Independent Research (The Sapere Aude programme), the Lundbeck Foundation, and the Villum foundation for financial support.

■ REFERENCES

(1) Grieshop, A. P.; Reynolds, C. C. O.; Kandlikar, M.; Dowlatabadi, H. A Black-carbon Mitigation Wedge. *Nat. Geosci.* **2009**, *2*, 533−534.

(2) Shindell, D.; et al. Simultaneously Mitigating Near-Term Climate Change and Improving Human Health and Food Security. *Science* **2012**, *335*, 183−189.

(3) Ramanathan, V.; Carmichael, G. Global and Regional Climate Changes Due to Black Carbon. *Nat. Geosci.* **2008**, *1*, 221−227.

(4) Hansen, J.; Nazarenko, L. Soot Climate Forcing via Snow and Ice Albedos. *Proc. Natl. Acad. Sci. U. S. A.* **2004**, *101*, 423−428.

(5) Heilbronner, E.; Weber, J.-P.; Michl, J.; Zahradník, R. The Electronic Spectra of Acenaphthylene and Fluoranthene. *Theor. Chim. Acta* **1966**, *6*, 141−158.
(6) Khalili, N. R.; Scheff, P. A.; Holsen, T. M. PAH Source Fingerprints for Coke Ovens, Diesel and, Gasoline Engines, Highway Tunnels, and Wood Combustion Emissions. *Atmos. Environ.* **1995**, *29*, 533−542.
(7) Maricq, M. M. Chemical Characterization of Particulate Emissions from Diesel Engines: A Review. *J. Aerosol Sci.* **2007**, *38*, 1079−1118.
(8) Mi, H.-H.; Lee, W.-J.; Chen, C.-B.; Yang, H.-H.; Wu, S.-J. Effect of Fuel Aromatic Content on PAH Emission from a Heavy-duty Diesel Engine. *Chemosphere* **2000**, *41*, 1783−1790.
(9) Granat, L.; Engström, J. E.; Praveen, S.; Rodhe, H. Light Absorbing Material (Soot) in Rainwater and in Aerosol Particles in the Maldives. *J. Geophys. Res., Atmos.* **2010**, *115*, D16307.
(10) Coz, E.; Leck, C. Morphology and State of Mixture of Atmospheric Soot Aggregates During the Winter Season Over Southern Asia-a Quantitative Approach. *Tellus B* **2011**, *63*, 107−116.
(11) Alexander, D. T. L.; Crozier, P. A.; Anderson, J. R. Brown Carbon Spheres in East Asian Outflow and Their Optical Properties. *Science* **2008**, *321*, 833−836.
(12) Christoffersen, T.; Hjorth, J.; Horie, O.; Jensen, N.; Kotzias, D.; Molander, L.; Neeb, P.; Ruppert, L.; Winterhalter, R.; Virkkula, A.; Wirtz, K.; Larsen, B. Cis-pinic Acid, a Possible Precursor for Organic Aerosol Formation from Ozonolysis of α-pinene. *Atmos. Environ.* **1998**, *32*, 1657−1661.
(13) Yassaa, N.; Peeken, I.; Zöllner, E.; Bluhm, K.; Arnold, S.; Spracklen, D.; Williams, J. Evidence for Marine Production of Monoterpenes. *Envir. Chem.* **2008**, *5*, 391−401.
(14) Luo, G.; Yu, F. A Numerical Evaluation of Global Oceanic Emissions of α-pinene and Isoprene. *Atmos. Chem. Phys.* **2010**, *10*, 2007−2015.
(15) Hede, T.; Leck, C.; Sun, L.; Tu, Y.; Ågren, H. A Theoretical Study Revealing the Promotion of Light-absorbing Carbon Particles Solubilization by Natural Surfactants in Nanosized Water Droplets. *Atmos. Sci. Lett.* **2013**, *14*, 86−90.
(16) Hede, T.; Li, X.; Leck, C.; Tu, Y.; Ågren, H. Model HULIS Compounds in Nanoaerosol Clusters - Investigations of Surface Tension and Aggregate Formation Using Molecular Dynamics Simulations. *Atmos. Chem. Phys.* **2011**, *11*, 6549−6557.
(17) Kohler, H. The Nucleus in and the Growth of Hygroscopic Droplets. *Trans. Faraday Soc.* **1936**, *32*, 1152−1161.
(18) Li, X.; Hede, T.; Tu, Y.; Leck, C.; Ågren, H. Surface-Active cis-Pinonic Acid in Atmospheric Droplets: A Molecular Dynamics Study. *J. Phys. Chem. Lett.* **2010**, *1*, 769−773.
(19) Tuckermann, R. Surface Tension of Aqueous Solutions of Water-Soluble Organic and Inorganic Compounds. *Atmos. Environ.* **2007**, *41*, 6265−6275.
(20) Frosch, M.; Prisle, N. L.; Bilde, M.; Varga, Z.; Kiss, G. Joint Effect of Organic Acids and Inorganic Salts on Cloud Droplet Activation. *Atmos. Chem. Phys.* **2011**, *11*, 3895−3911.
(21) Baheti, A.; Lee, C.-P.; Thomas, K. R. J.; Ho, K.-C. Pyrene-based Organic Dyes with Thiophene Containing π -Linkers for Dye-Sensitized Solar Cells: Optical, Electrochemical and Theoretical Investigations. *Phys. Chem. Chem. Phys.* **2011**, *13*, 17210−17221.
(22) Venkatramaiah, N.; Kumar, S.; Patil, S. Femtogram Detection of Explosive Nitroaromatics: Fluoranthene-Based Fluorescent Chemosensors. *Chem.—Eur. J.* **2012**, *18*, 14745−14751.
(23) Wolfbeis, O.; Leiner, M. Recent Progress in Optical Oxygen Sensing. *Proc. SPIE* **1988**, *906*, 42−48.
(24) Sharma, A.; Wolfbeis, O. S. The Quenching of the Fluorescence of Polycyclic Aromatic Hydrocarbons and Rhodamine 6G by Sulphur Dioxide. *Spectrochim. Acta A* **1987**, *43*, 1417−1421.
(25) Enomoto, S.; Hasegawa, M.; Yoshinaga, T.; Hiratsuka, H.; Kobayashi, M.; Okubo, J.; Hoshi, T. Dispersion Interaction between Fluoranthene and Benzene in Cyclohexane. *Bull. Chem. Soc. Jpn.* **2002**, *75*, 689−693.
(26) Malloci, G.; Mulas, G.; Joblin, C. Electronic Absorption Spectra of PAHs up to Vacuum UV. *A&A.* **2004**, *426*, 105−117.
(27) Hess, B.; Kutzner, C.; van der Spoel, D.; Lindahl, E. GROMACS 4: Algorithms for Highly Efficient, Load-Balanced, and Scalable Molecular Simulation. *J. Chem. Theory Comput.* **2008**, *4*, 435−447.
(28) Pronk, S.; Páll, S.; Schulz, R.; Larsson, P.; Bjelkmar, P.; Apostolov, R.; Shirts, M.; Smith, J.; Kasson, P.; van der Spoel, D.; Hess, B.; Lindahl, E. GROMACS 4.5: a High-Throughput and Highly Parallel Open Source Molecular Simulation Toolkit. *Bioinformatics* **2013**, *7*, 845−854.
(29) Berendsen, H. J. C.; Grigera, J. R.; Straatsma, T. P. The Missing Term in Effective Pair Potentials. *J. Phys. Chem.* **1987**, *91*, 6269−6271.
(30) Nosé, S. A Molecular Dynamics Method for Simulation in the Canonical Ensemble. *Mol. Phys.* **1984**, *52*, 255−268.
(31) Hess, B.; Bekker, H.; Berendsen, H. J. C.; Fraaije, J. G. E. M. LINCS: A Linear Constraint Solver for Molecular Simulations. *J. Comput. Chem.* **1997**, *18*, 1463−1472.
(32) Jorgensen, W. L.; Maxwell, D. S.; Tirado-Rives, J. Development and Testing of the OPLS All-Atom Force Field on Conformational Energetics and Properties of Organic Liquids. *J. Am. Chem. Soc.* **1996**, *118*, 11225−11236.
(33) Filippo De Angelis, A. S.; Fantacci, S. Theoretical Modeling of Spectroscopic Properties of Molecules in Solution: Toward an Effective Dynamical Discrete/Continuum Approach. *Theor. Chem. Acc.* **2007**, *117*, 1013−1104.
(34) De Mitri, N.; Monti, S.; Prampolini, G.; Barone, V. Absorption and Emission Spectra of a Flexible Dye in Solution: A Computational Time-Dependent Approach. *J. Chem. Theory Comput.* **2013**, *9*, 4507−4516.
(35) Aidas, K.; Kongsted, J.; Osted, A.; Mikkelsen, K. V.; Christiansen, O. Coupled Cluster Calculation of the n → π^* Electronic Transition of Acetone in Aqueous Solution. *J. Phys. Chem. A* **2005**, *109*, 8001−8010.
(36) Murugan, N. A.; Kongsted, J.; Rinkevicius, Z.; Aidas, K.; Ågren, H. Modeling the Structure and Absorption Spectra of Stilbazolium Merocyanine in Polar and Nonpolar Solvents Using Hybrid QM/MM Techniques. *J. Phys. Chem. B* **2010**, *114*, 13349−13357.
(37) Murugan, N. A.; Kongsted, J.; Rinkevicius, Z.; Ågren, H. Demystifying the Solvatochromic Reversal in Brooker's Merocyanine Dye. *Phys. Chem. Chem. Phys.* **2011**, *13*, 1290−1292.
(38) Rajamani, R.; Gao, J. Combined QM/MM Study of the Opsin Shift in Bacteriorhodopsin. *J. Comput. Chem.* **2002**, *23*, 96−105.
(39) Murugan, N. A.; Kongsted, J.; Rinkevicius, Z.; Ågren, H. Color Modeling of Protein Optical Probes. *Phys. Chem. Chem. Phys.* **2012**, *14*, 1107−1112.
(40) Murugan, N. A.; Olsen, J. M. H.; Kongsted, J.; Rinkevicius, Z.; Aidas, K.; Ågren, H. Amyloid Fibril-Induced Structural and Spectral Modifications in the Thioflavin-T Optical Probe. *J. Phys. Chem. Lett.* **2013**, *4*, 70−77.
(41) Steindal, A. H.; Olsen, J. M. H.; Ruud, K.; Frediani, L.; Kongsted, J. A Combined Quantum Mechanics/Molecular Mechanics Study of the One- and Two-Photon Absorption in the Green Fluorescent Protein. *Phys. Chem. Chem. Phys.* **2012**, *14*, 5440−5451.
(42) Aidas, K.; et al. The Dalton Quantum Chemistry Program System. *WIREs Comput. Mol. Sci.* **2014**, DOI: 10.1002/wcms.1172.
(43) Olsen, J. M.; Aidas, K.; Kongsted, J. Excited States in Solution through Polarizable Embedding. *J. Chem. Theor. Comput.* **2010**, *6*, 3721−3734.
(44) Olsen, J. M.; Kongsted, J. Molecular Properties through Polarizable Embedding. *Adv. Quantum Chem.* **2011**, *61*, 107−143.
(45) Bayly, C. I.; Cieplak, P.; Cornell, W.; Kollman, P. A. A Well-Behaved Electrostatic Potential Based Method Using Charge Restraints for Deriving Atomic Charges: the RESP Model. *J. Phys. Chem.* **1993**, *97*, 10269−10280.
(46) Dunning, T. H. J. Gaussian Basis Sets for Use in Correlated Molecular Calculations. I. The Atoms Boron Through Neon and Hydrogen. *J. Chem. Phys.* **1989**, *90*, 1007−1023.
(47) Frisch, M. J.; et al. *Gaussian 09*, Revision A.02; Gaussian, Inc.: Wallingford, CT, 2009.

(48) Wang, J.; Wang, W.; Kollman, P. A.; Case, D. A. Automatic Atom Type and Bond Type Perception in Molecular Mechanical Calculations. *J. Mol. Graphics Modell.* **2006**, *25*, 247−260.
(49) Gagliardi, L.; Lindh, R.; Karlström, G. Local Properties of Quantum Chemical Systems: the LoProp Approach. *J. Chem. Phys.* **2004**, *121*, 4494−4500.
(50) Ahlström, P.; Wallqvist, A.; Engström, S.; Jönsson, B. A Molecular Dynamics Study of Polarizable Water. *Mol. Phys.* **1989**, *68*, 563−581.
(51) Yanai, T.; Tew, D. P.; Handy, N. C. A New Hybrid Exchange-Correlation Functional Using the Coulomb-Attenuating Method (CAM-B3LYP). *Chem. Phys. Lett.* **2004**, *393*, 51−57.
(52) Peach, M. J. G.; Helgaker, T.; Sałek, P.; Keal, T. W.; Lutnæs, O. B.; Tozer, D. J.; Handy, N. C. Assessment of a Coulomb-Attenuated Exchange-Correlation Energy Functional. *Phys. Chem. Chem. Phys.* **2006**, *8*, 558−562.
(53) Schafer, A.; Huber, C.; Ahlrichs, R. Fully Optimized Contracted Gaussian Basis Sets of Triple Zeta Valence Quality for Atoms Li to Kr. *J. Chem. Phys.* **1994**, *100*, 5829−5835.
(54) Christiansen, O.; Koch, H.; Jørgensen, P. The Second-Order Approximate Coupled Cluster Singles and Doubles Model CC2. *Chem. Phys. Lett.* **1995**, *243*, 409−418.
(55) Tomasi, J.; Mennucci, B.; Cammi, R. Quantum Mechanical Continuum Solvation Models. *Chem. Rev.* **2005**, *105*, 2999−3094.
(56) Schwabe, T.; Sneskov, K.; Haugaard Olsen, J. M.; Kongsted, J.; Christiansen, O.; Httig, C. PERI-CC2: A Polarizable Embedded RI-CC2Method. *J. Chem. Theory Comput.* **2012**, *8*, 3274−3283.
(57) Hub, J. S.; Caleman, C.; van der Spoel, D. Organic Molecules on the Surface of Water Droplets - an Energetic Perspective. *Phys. Chem. Chem. Phys.* **2012**, *14*, 9537−9545.
(58) Cappa, C. D.; et al. Radiative Absorption Enhancements Due to the Mixing State of Atmospheric Black Carbon. *Science* **2012**, *337*, 1078−1081.